

Measurements of light transmission in deep Sea with the *AC9* trasmissometer

A. Capone^{a,b}, T. Digaetano^c, A. Grimaldi^d, R. Habel^e,
 D. Lo Presti^d, E. Migneco^{f,g}, R. Masullo^a, F. Moro^c,
 M. Petrucci^b, C. Petta^g, P. Piattelli^f, N. Randazzo^d,
 G. Riccobene^{f,*}, E. Salusti^b, P. Sapienza^f, M. Sedita^f,
 L. Trasatti^h and L. Ursella^c.

^a*Dipartimento di Fisica Università La Sapienza, P.le A. Moro 2, 00185, Roma, Italy*

^b*INFN Sezione Roma-1, P.le A. Moro 2, 00185, Roma, Italy*

^c*Dipartimento di Oceanografia Fisica, Osservatorio Geofisico Sperimentale, Borgo Grotta Gigante 42C, 34016, Sgonico (TS), Italy*

^d*INFN Sezione Catania, Corso Italia 57, 95129, Catania, Italy*

^e*Dipartimento di Fisica Università di Cagliari and Sezione INFN Cagliari, 09042, Monserrato (CA), Italy*

^f*Laboratori Nazionali del Sud INFN, Via S.Sofia 44, 95123, Catania, Italy*

^g*Dipartimento di Fisica e Astronomia Università di Catania*

^h*Laboratori Nazionali di Frascati INFN, Via Enrico Fermi 40, 00044, Frascati (RM), Italy*

Abstract

The NEMO Collaboration aims to construct an underwater Čerenkov detector in the Mediterranean Sea, able to act as a neutrino telescope. One of the main tasks of this project, which implies difficult technological challenges, is the selection of an adequate marine site. In this framework the knowledge of light transmission properties in deep seawater is extremely important. The collaboration has measured optical properties in several marine sites near the Italian coasts, at depths >3000 m, using a set-up based on a *AC9*, a commercial trasmissometer, manufactured by *WETLabs*. The results obtained for the two sites reported in this paper (*Alicudi* and *Ustica*), show that deep seawater optical properties are comparable to those of the clearest waters.

Key words: neutrino telescope, NEMO, attenuation, absorption, deep sea
PACS: 95.55.Vj, 29.40.Ka, 92.10.Pt, 07.88.+y

1 Overview

The observation of Ultra High Energy Cosmic Rays (UHECR) with energy higher than 10^{20} eV has attracted the attention of the astrophysics and particle-physics community on the most energetic phenomena taking place in the Universe. It is supposed that such energetic particles are accelerated in extragalactic sources.

Gamma ray sources with energy up to tens of TeV have also been observed. If high energy photons are generated through the production and decay of neutral pions, it is reasonable to expect, from the same sources, an associated flux of high energy neutrinos, generated through the production and decay of charged pions. Along their journey in the universe, most part of the electromagnetic and hadronic emission is deflected or absorbed by the electromagnetic background and by the intergalactic and interstellar matter. Neutrinos, on the contrary, are not significantly absorbed by the intergalactic medium and are not deflected by the intergalactic magnetic fields. Already in 1960 Markov (1; 2) proposed to use seawater as a huge target to detect UHE neutrinos, looking at their charged current weak interactions. The outgoing lepton generates, along its path in seawater, Čerenkov light that can be detected by a lattice of optical sensors. The reconstruction of the muon track, and thus of the neutrino direction, offers the possibility to identify the neutrino sources opening the new exciting field of neutrino astronomy. The observation of high energy neutrino fluxes expected from astrophysical sources requires a detector with an effective area close to 10^6 m² instrumented along a distance comparable to the range in water (\sim km) of the high energy muons (\sim 1000 TeV). The identified neutrino sources identified could be catalogued in the sky map and eventually compared with the known gamma sources. The construction of a detector of such dimensions, usually called a km³ Neutrino Telescope, is one of the main challenges of astroparticle physics today. The Mediterranean Sea offers optimal conditions, on a worldwide scale, to locate an underwater neutrino telescope. The choice of the km³ scale neutrino telescope location is such an important task that careful studies of candidate sites must be carried out in order to identify the most suitable one. Along the Italian coasts several sites exist, at depth 3300 \div 3500 m, that are potentially interesting to host an undersea neutrino telescope. In these sites we have studied deep seawater optical properties (absorption and attenuation) and environmental properties: water temperature and salinity, biological activity, water currents, sedimentation. In this paper we report light transmission measurements carried out in two sites named *Ustica* (during November 1999) and *Alicudi* (on December 1999), in the Southern Tyrrhenian Sea, located at:

* Fax: +39 095 542 271

Email address: riccobene@lns.infn.it (G. Riccobene).

- 39°05' N 13°20' E, North-Est of Ustica island;
- 39°05' N 14°20' E, North of Alicudi island.

2 Optical properties of deep sea

Water transparency to electromagnetic radiation can be characterized by means of quantitative parameters: the absorption length L_a and the scattering length L_b . Each length represents the path after which a photon beam of intensity I_0 at wavelength λ , travelling along the emission direction, is reduced to $1/e$ by absorption or diffusion phenomena. These quantities can be directly derived by the simple relation:

$$I(x, \lambda) = I_0(\lambda)e^{-\frac{x}{L(\lambda)}}, \quad (1)$$

where x is the optical path traversed by the beam and I_0 the source intensity. In literature absorption ($a = 1/L_a$) and scattering ($b = 1/L_b$) coefficients are extensively used to characterize the light transmission in matter as well as the attenuation coefficient (c) defined as:

$$c(\lambda) = a(\lambda) + b(\lambda). \quad (2)$$

The main cause of light absorption in water is excitation of vibrational states of the water molecule by photons (3; 4; 5): due to such process the photon energy is entirely deposited in the traversed medium. Scattering refers to processes in which the direction of the photon is changed without any other alteration. Scattering phenomena in which the photon wavelength changes (e.g. Raman effect) happen less frequently. Scattering can take place either on molecules (Rayleigh scattering) or on dissolved particulate (Mie scattering).

In pure water, light absorption and scattering are strongly wavelength dependent. In particular light transmission in pure water is extremely favored in the range $350 \div 550$ nm, overlapping the region in which PMTs usually reach the highest quantum efficiency. In the visible region of the electromagnetic spectrum light absorption steeply decreases as a function of wavelength and reaches its minimum at about 420 nm (see figure 2). This is the reason why seawater has a blue-green color.

The optical properties of natural seawater are functions of water salinity, water temperature and of the concentration of dissolved organic and inorganic matter. Light absorption and diffusion in water as a function of salinity and temperature have been extensively studied (7). It has been noticed that, for $\lambda \geq 400$ nm, the dependence of scattering coefficient on temperature and

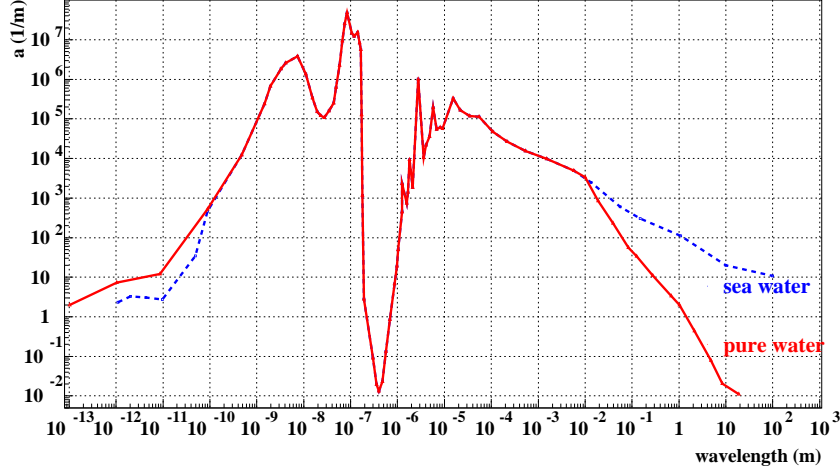


Fig. 1. Absorption coefficient of electromagnetic waves for pure and seawater as function of wavelength. Data taken from Mobley (6).

salinity is negligible while the variation of the absorption coefficient is significant, in particular at $\lambda > 710$ nm (for details see §7). The seawater diffusion and absorption coefficients can be parameterized as the sum of a term due to optically pure water (i.e. water without dissolved particulate) at defined conditions of temperature and salinity ($a_W^{T,S}$, $b_W^{T,S}$), and a term that accounts for interaction of light with particulate (a_p , b_p):

$$a_{SW}(\lambda) = a_W^{T,S}(\lambda) + a_p(\lambda), \quad (3)$$

$$b_{SW}(\lambda) = b_W^{T,S}(\lambda) + b_p(\lambda). \quad (4)$$

Optical measurements of deep seawater have shown that the presence of particulate has a negligible effect on light absorption but it enlarges the light diffusion coefficient. Since water temperature and salinity and particulate concentration may vary significantly in different marine sites it is extremely important to measure optical parameters *in situ*.

3 The AC9 transmissometer

We performed attenuation and absorption measurements of light in deep seawater by means of a set-up based on a transmissometer: the *AC9* manufactured by *WETLabs* (8). The device compactness (68 cm height \times 10.2 cm diameter) and its pressure resistance (it can operate down to 6000 m depth) are excellent for our purposes. The *AC9* performs attenuation and absorption measurements independently using two different light paths and spanning the light spectrum over nine different wavelengths (412, 440, 488, 510, 532, 555, 650, 676, 715

nm). In our measurements we obtain an accuracy in $a(\lambda)$ and $c(\lambda)$ of about $1.5 \cdot 10^{-3} \text{ m}^{-1}$.

The *AC9* attenuation and absorption measurement technique is based on the Lambert's law of collimated beams (see equation 1) where x is the beam path-length, $I_0(\lambda)$ is the intensity of the collimated primary beam, at a given wavelength λ , and $I(x, \lambda) = I_{a,c}(x, \lambda)$ is the beam intensity measured at distance x , as a result of absorption or attenuation effect respectively.

In order to produce collimated monochromatic light beams, the instrument is equipped with an incandescence lamp and a set of collimators and nine monochromatic ($\Delta\lambda \sim 10 \text{ nm}$) filters. Two different beams are available at the same time for independent measurements of attenuation and absorption. Each beam is split in two parts by a mirror: the reflected one reaches a reference silicon photon detector. The refracted one crosses a quartz window and enters inside a 25 cm long pipe. During deep sea measurements seawater fills the pipes (*flow tubes*). The flow tube used for attenuation measurements has a black inner surface in order to absorb all photons scattered by seawater. A collimated silicon photon detector (angular acceptance $\sim 0.7^\circ$) is placed at the end of the path, along the source axis. Thanks to this strongly collimated layout the end-path detector receives only photons which have not interacted (neither absorbed nor scattered). The reference detector measures the source intensity $I_0(\lambda)$, the end-path detector measures the attenuated beam intensity $I_c(x, \lambda)$, x is the known beam path in water (0.25 m). The attenuation coefficient is therefore calculated as:

$$c(\lambda) = \frac{1}{x} \ln \frac{I_0(\lambda)}{I_c(x, \lambda)}. \quad (5)$$

In the absorption channel, the inner surface of the *absorption flow tube* behaves like a cylindrical mirror. The light scattered by seawater is reflected and redirected towards a wide angular acceptance silicon photon detector. In first approximation all scattered photons are detected and the ratio between the intensities $I_0(\lambda)$ and $I_a(x, \lambda)$ is only a function of the seawater absorption coefficient $a(\lambda)$.

Using *AC9* data, the scattering coefficient can be calculated by subtracting the absorption value from the attenuation value at each given wavelength (see equation 2).

4 AC9 measurements principles

In the interval of wavelength interesting for a Čerenkov neutrino telescope, $\lambda = 350 \div 550$ nm, the expected values of absorption and attenuation coefficients in deep seawater are $\sim 10^{-2} \text{ m}^{-1}$, very close to the pure water ones. This implies that the instrument should have sensitivity and accuracy of the order of $1 \div 2 \cdot 10^{-3} \text{ m}^{-1}$. The calibration of the instrument plays the most important role in determining the accuracy in measurements. In the above defined wavelength range, pure water optical properties have been extensively measured, therefore pure water can be assumed as a reference medium (10; 11).

Instrumental effects - such as the status of optical windows, of the electronics, etc.- can also be studied filling the flow tubes with a medium with a negligible light absorption and attenuation (e.g. dry air or N_2).

The instrument calibration can be, thus, performed and tested any time filling the flow tubes with a medium with known optical properties: either pure water (*pure water calibration*) or N_2 (*air calibration*). Filling the flow tubes with pure water we measure, for example in the absorption channel, the values:

$$a(\lambda) = a_I(\lambda) + a_{PW}(\lambda) \quad (6)$$

and, in the case of N_2 ,

$$a(\lambda) = a_I(\lambda) + a_{N_2}(\lambda). \quad (7)$$

The extra-term $a_I(\lambda)$ takes into account the light absorption in the instrument optics (that is function of the status of quartz windows and mirror surfaces) and all other instrumental effects (see §7). This means that this term can vary with time and can be a function of the internal electronics temperature. The same argument is valid for the attenuation channel.

With pure water inside the flow tubes the measurement of *AC9* can be set equal to the known values of $a_{PW}(\lambda)$ and $c_{PW}(\lambda)$. The result of the *water calibration* procedure is a set of 18 calibration constants (for the nine absorption and attenuation channels) that represent the working status of *AC9*. The *AC9* internal software subtracts these coefficients to the actual reading of the instrument such that each *AC9* output value, when reference water fills the flow tubes, should be equal to zero.

Filling the flow-tubes with sea water we measure:

$$a(\lambda) = a_I(\lambda) + a_{SW}(\lambda) \quad (8)$$

Table 1

Absorption and attenuation coefficients (in units of 10^{-3}) of pure water at $T = 25^\circ$ referenced in the *AC9* manual (8) and (9)

λ (nm)	412	440	488	510	532	555	650	676	715
a (10^{-3} m^{-1})	5.4	8.3	17.7	38.2	51.6	69.0	359.4	441.6	1049.2
c (10^{-3} m^{-1})	9.7	11.9	20.0	40.2	53.3	70.4	360.1	442.2	1049.7

$$c(\lambda) = c_I(\lambda) + c_{SW}(\lambda). \quad (9)$$

Then the values of *AC9* output corresponding to the case of deep sea water filling the flow tubes are:

$$\Delta a_{SW}(\lambda) = a_{SW}(\lambda) - a_{PW}(\lambda), \quad (10)$$

$$\Delta c_{SW}(\lambda) = c_{SW}(\lambda) - c_{PW}(\lambda). \quad (11)$$

5 AC9 calibration procedure

The *AC9* manufacturer (*WETLabs*) provides the instrument calibration performed with de-ionized and de-gassed pure water, at given temperature (25°C), as referenced in (10; 11). The optical properties of this medium, at the nine wavelengths relevant for the *AC9*, are listed in table 1. *Wetlabs* provides also the results of the instrument calibration performed with dry air. The set of constants that relate the *water calibration* values to the *air calibration* ones are provided by *WETLabs*.

In principle, in order to test, from time to time, the validity of the used set of *water calibration* constants, the user should check the *AC9* response after filling the flow tubes with pure water in *reference* conditions. However, since pure water is not easily available during cruises, we check the calibration of the *AC9* in dry air testing the validity of air calibration constants after having filled the flow tubes with high purity grade N_2 . We extensively perform these operations during naval campaigns before every deployment.

We have accurately studied the dependence of *air calibration* constants as a function of *AC9* internal temperature. We noticed that during measurement in the Mediterranean Sea, where at depth > 1500 m the water temperature is $\sim 13 \div 14^\circ\text{C}$, the *AC9* internal temperature stabilizes at $T_{AC9} \sim 22.5^\circ\text{C}$. To reduce the systematic error in the knowledge of the instrument calibration constants, during checks of *air calibration* we keep the internal *AC9* temperature at $\sim 22.5^\circ\text{C}$ by means of a refrigerator. Figure 2 shows some *AC9* measured raw values $\Delta a_{N_2}(\lambda)$, $\Delta c_{N_2}(\lambda)$ (analogous to $\Delta a_{SW}(\lambda)$ and $\Delta c_{SW}(\lambda)$)

as defined in equations 10 and 11), as a function of T_{AC9} , obtained checking the *air calibration* just before the first deployment in *Alicudi* site. In the range $22^\circ\text{C} < T_{AC9} < 23^\circ\text{C}$ the $\Delta a_{N_2}(\lambda)$, $\Delta c_{N_2}(\lambda)$ average values are close to zero and RMS are of the order of $1.5 \cdot 10^{-3} \text{ m}^{-1}$. These average values (that we call $a_{N_2}^{off}(\lambda)$ and $c_{N_2}^{off}(\lambda)$) are used as *offsets* and subtracted during off-line data analysis, as described in the following sections.

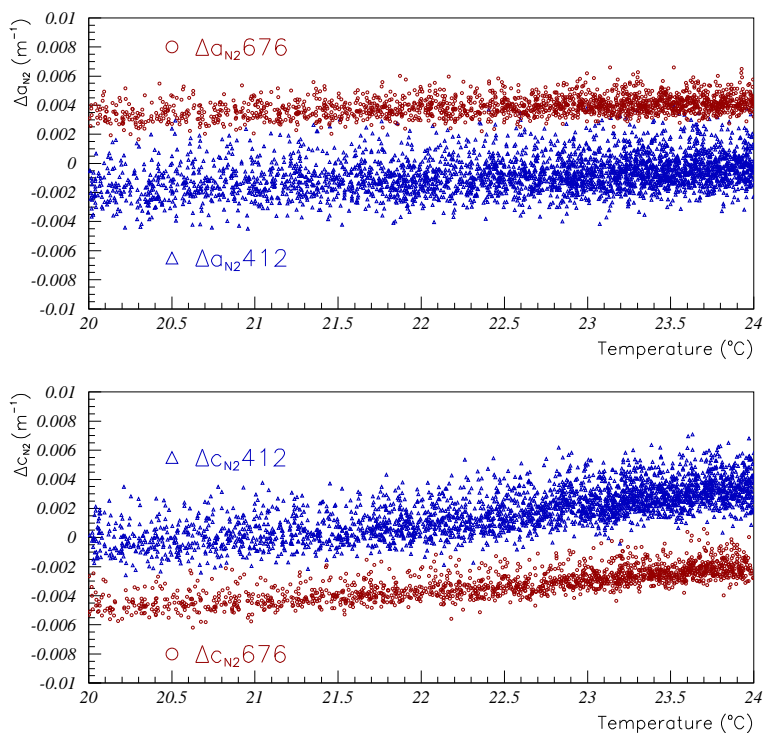


Fig. 2. Absorption $\Delta a_{N_2}(\lambda)$ and attenuation $\Delta c_{N_2}(\lambda)$ raw values for $\lambda = 412, 676$ nm, measured, as function of the *AC9* internal temperature, during a dry air calibration before the first measurement in *Alicudi* site.

6 Deep Sea Setup

During deep sea measurements the *AC9* is connected to a standard oceanographic CTD (Conductivity Temperature Depth) probe, the *Ocean MK-317* manufactured by *IDRONAUT*. A pump is used to ensure re-circulation of seawater inside the *AC9* pipes. The *AC9* and the pump are powered by a 14 V battery pack. In figure 3 we show the whole set-up mounted on an AISI-316 stainless-steel cage before a deployment.

When the system is in operation, the *RS-232* stream of the *AC9* data is converted into *FSK* stream by a modem card placed inside the CTD. Data are



Fig. 3. Deployment of AC9 deep-sea setup.

sent to sea surface through an electro-mechanical cable, that is also used to transmit power to CTD (~ 1 A at 30 VDC). The data acquisition system permits both the *AC9* data telemetry and the data storage on a PC onboard the ship. The CTD data (depth, water salinity and temperature) are recorded on a local memory. Both instruments also record an absolute time information, which is used to couple the *AC9* and the CTD data during off-line analysis. This procedure allows to relate water optical properties to depth, water salinity and temperature. The CTD-*AC9* acquisition program gives about six measurements per second, usually we deploy the set-up at speed of 1 m/s. In figure 4 we show, as function of depth, water salinity and temperature together with the final absolute values of absorption and attenuation coefficient for $\lambda = 440$ nm measured during the first (black dots) and the second (red dots) deployments in Alicudi site. As it appears in the figure, the layer composition of Tyrrhenian Sea, well studied by oceanologists in terms of salinity and temperature, is also indicated by the measurements of water optical properties: the *AC9* sensitivity permits to distinguish layers of water where absorption and attenuation coefficients vary for $\sim 1 \cdot 10^{-3} \text{ m}^{-1}$.

7 Data Analysis

In order to obtain the values of deep seawater absorption and attenuation coefficients from the measured raw values we need to apply few corrections. The

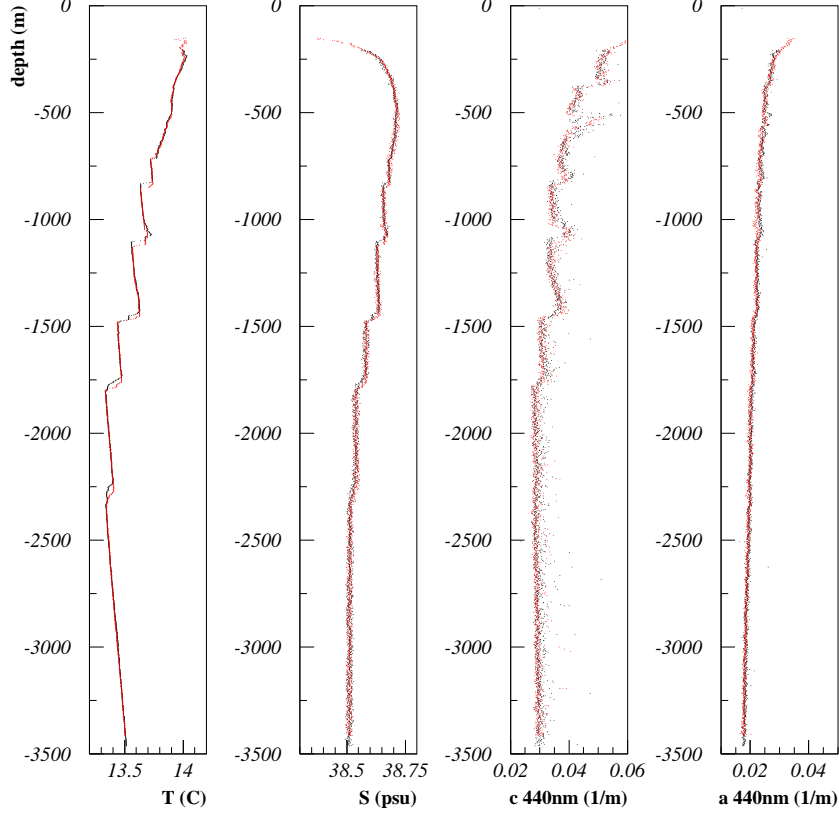


Fig. 4. Temperature, salinity, attenuation and absorption coefficients (at $\lambda = 440$ nm) as a function of depth, measured in the first (black) and in the second (red) deployment in *Alicudi* site. The values measured in the two deployments are nearly superimposed in the figure.

first correction consists in removing the set of calibration constants $a_{N_2}^{off}(\lambda)$, $c_{N_2}^{off}(\lambda)$ described in §5:

$$\Delta a'(\lambda) = \Delta a_{raw}(\lambda) - a_{N_2}^{off}(\lambda), \quad (12)$$

$$\Delta c'(\lambda) = \Delta c_{raw}(\lambda) - c_{N_2}^{off}(\lambda). \quad (13)$$

Further corrections for the attenuation channel could be needed to take into account that the silicon photon detector in the attenuation channel has a finite angular acceptance (0.7°) and that the inner surface of the *attenuation flow tube* does not behave as a perfect absorber. These two corrections have been evaluated to be much lower than $1.5 \cdot 10^{-3} \text{ m}^{-1}$ that we quote as systematic error associated to the result. Therefore $\Delta c_{corr}(\lambda) = \Delta c'(\lambda)$.

The absolute values of the light attenuation coefficients in seawater (as a function of depth) can be finally obtained inverting equations 11.

Concerning the absorption channel, up to now, we considered that the inner surface of the *flow tube* is perfectly reflecting. This assumption is valid only

in first approximation and a proper correction has to be applied to the measured raw values. If the inner mirror is not perfectly reflecting, in presence of light scattering, a fraction of the diffused photons do not reach the end-path detector. We now illustrate how we have evaluated the amount of this effect using *AC9* data collected for $\lambda > 650$ nm.

Photon diffusion in the absorption channel is also present when the tube is filled with pure water. This implies that, with the described calibration procedure, part of the effect is already accounted for at the calibration time, i.e. the effect of photons diffused at large angle by Rayleigh scattering on molecules.

The presence of particulate in deep seawater results as an additional cause of absorption and diffusion processes; but, at red and infrared wavelengths, the absorption due to the particulate present in deep seawater is negligible (12). It follows that the values $\Delta a'(\lambda)$ at $\lambda = 676$ nm and $\lambda = 715$ nm, measured by the *AC9* in deep seawater, allow us to evaluate the effect of the not perfect reflectivity of the *absorption flow tube* mirror.

Actually a value of $\Delta a'(\lambda) \neq 0$ for seawater has to be expected because of the presence of salts and because deep seawater temperature ($\sim 13 \div 14^\circ\text{C}$ in the deep Mediterranean Sea) is not equal to the calibration water temperature (25°C). The dependence of light absorption and diffusion in water as a function of salinity and temperature has been extensively studied (7). It has been noticed that, for $\lambda > 400$ nm, the dependence of $b_W^{T,S}(\lambda)$ on temperature and salinity is negligible; on the contrary the variation of the absorption coefficient can be expressed by the equation:

$$\Delta a^{T,S}(\lambda) = [\Psi_T \cdot (T - T_{ref}) + \Psi_S \cdot (S - S_{ref})] \quad (14)$$

where $T_{ref} = 25^\circ\text{C}$, $S_{ref} = 0$ practical salinity units (p.s.u.), T and S are the actual values of seawater. The constants Ψ_T and Ψ_S are known as a function of the wavelength (7; 12): for $\lambda = 676$ nm the values are $\Psi_T(676) = 1 \cdot 10^{-4} \text{ m}^{-1} \text{ }^\circ\text{C}^{-1}$ and $\Psi_S(676) = 8 \cdot 10^{-5} \text{ m}^{-1} \text{ p.s.u.}^{-1}$. The slope of the temperature corrections for $\lambda = 715$ nm is much larger: $\Psi_T(715) = 2.9 \cdot 10^{-3} \text{ m}^{-1} \text{ }^\circ\text{C}^{-1}$ (while $\Psi_S(715) = -8 \cdot 10^{-5} \text{ m}^{-1} \text{ p.s.u.}^{-1}$).

We evaluate the correction due to the internal mirror of the *absorption flow tube* only at $\lambda = 676$ nm since the uncertainty on the temperature correction at this wavelength is smaller.

The evaluation of the contribution to the value of $\Delta a'(676)$ due to the photons diffused by particulate and not reflected toward the end-path detector is determined by means of the equation:

$$\Delta a^{mirror}(676) = \Delta a'(676) - \Delta a^{T,S}(676). \quad (15)$$

The measurement of S_{SW} and T_{SW} , made by the CTD (see §6), allows to evaluate the correction $\Delta a^{mirror}(676)$ as a function of depth.

It has been suggested (13) that the shape and magnitude of the Mie volume scattering function, in first approximation, can be considered almost independent on wavelength for the interval of λ in which the *AC9* operates: the correction due to the *mirror* effect is, therefore, independent on wavelength. It turns out that $\Delta a^{mirror}(676)$ can be used to correct the measured values of absorption coefficients for all wavelengths. Applying this correction we obtain:

$$\Delta a_{corr}(\lambda) = \Delta a'(\lambda) - \Delta a^{mirror}(676). \quad (16)$$

Finally, adding the pure water absorption (a_{PW}) and attenuation (c_{PW}) coefficients to the obtained Δa_{corr} and $\Delta c_{corr}(\lambda)$, we evaluate (as a function of depth) the seawater *inherent optical properties*:

$$a_{SW}(\lambda) = \Delta a_{corr}(\lambda) + a_{PW}(\lambda), \quad (17)$$

$$c_{SW}(\lambda) = \Delta c_{corr}(\lambda) + c_{PW}(\lambda). \quad (18)$$

Figure 5, that refers to the second measurement in Alicudi site, illustrates the analysis procedure for $\lambda = 412$ nm. As function of depth, we show the raw measured values of the absorption and attenuation coefficients (black dots), the values obtained applying the *offset* correction (red dots) and the *mirror* correction (blue dots) for $a_{SW}(412)$ and $c_{SW}(412)$.

The same analysis has been applied to the values measured at $\lambda = 440, 488, 510, 532, 650, 676$ and 715 nm. The values of $a_{SW}(\lambda)$ and $c_{SW}(\lambda)$ measured in the four deployments carried out in *Alicudi* and *Ustica* show very good agreement.

We do not show results for $\lambda = 555$ nm due to a temporary hardware problem happened to the interferometric filter during the naval campaign.

In the following we will quantify the optical properties of deep seawater averaging the absorption and attenuation coefficients in the range of depth interesting for a km^3 neutrino detector: a 400 m wide interval, with its base ~ 150 m above the seabed.

In figure 6 we show, as an example, the distribution of $a_{SW}(412)$ and $c_{SW}(412)$ values, averaged for each meter, in the interval of depth $2850 \div 3250$ m, related to the deployments in *Ustica* and *Alicudi* (seabed depth ~ 3400 m for both sites).

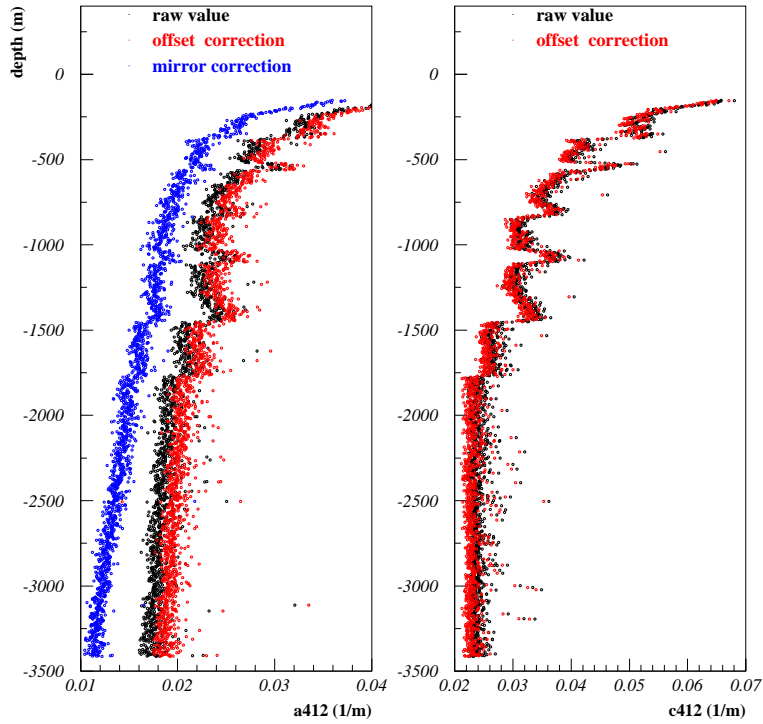


Fig. 5. Raw values (black dots) of the absorption and attenuation coefficients at 412 nm. The figure also shows the values obtained after *offset correction* (red dots) and, only in the case of absorption, the values after *mirror correction* (blue dots).

In table 7 we list the average values of the distributions of $\Delta a_{corr}(\lambda)$ and $\Delta c_{corr}(\lambda)$ in the same interval of depth.

The statistical errors associated to these values are evaluated from the RMS of the distributions (see, for example, figure 6). The systematic errors, mainly due to the accuracy of the calibration check procedure, have been evaluated to be equal to $1.5 \cdot 10^{-3}$. The absolute ($a_{SW}(\lambda), c_{SW}(\lambda)$) values can be obtained adding the values of attenuation and absorption of the *reference* water (see equations 17,18 and table 1).

Finally, we present in figure 7 the values of absorption and attenuation lengths, as a function of wavelength, for the same interval of depth.

8 Discussion

The importance of measuring seawater optical properties *in situ* has been discussed by several authors. The set-up we used permits to evaluate seawater

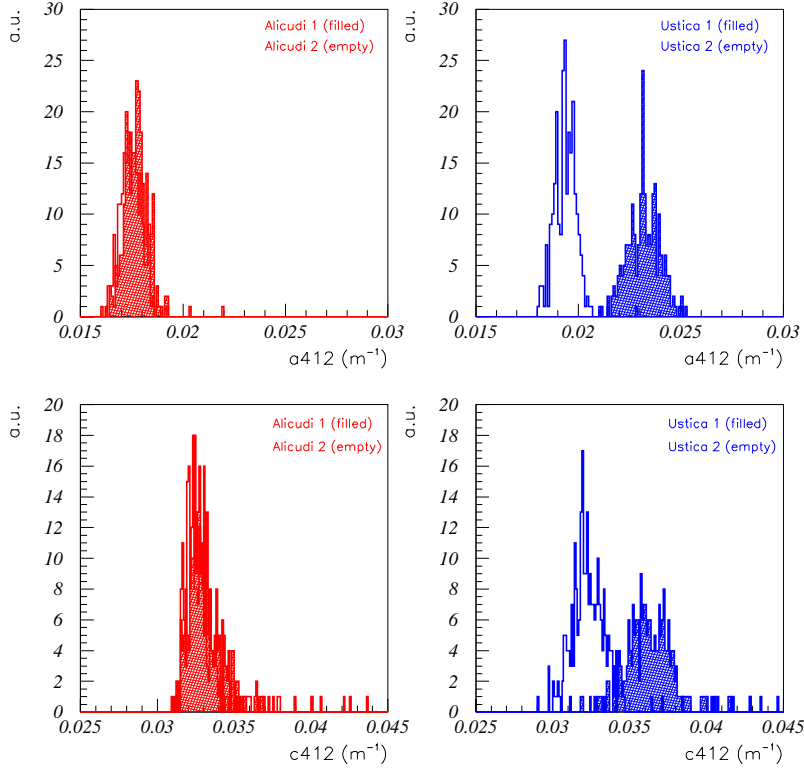


Fig. 6. Distributions of the absorption and attenuation coefficients, at $\lambda = 412$ nm, measured in *Alicudi* and *Ustica* in the depth interval $2850 \div 3250$ m. The results for a_{412} and c_{412} for the two measurements in *Alicudi* are in excellent agreement and appear nearly superimposed in the figure.

light absorption and attenuation coefficient as a function of depth and wavelength (in the range $412 \div 715$ nm). Accurate calibration checks allow us to obtain an accuracy in the evaluation of $a(\lambda)$ and $c(\lambda)$ of the order of $1.5 \cdot 10^{-3} \text{ m}^{-1}$.

The values of $a_{SW}(\lambda)$ measured in the depth interval of interest in *Alicudi* and *Ustica* are very close to the ones reported by Smith and Baker as *pure seawater* absorption (14). The discrepancy is less than $\sim 5 \cdot 10^{-3} \text{ m}^{-1}$ at all wavelengths, except at 715 nm where the temperature effect is relevant. Average absorption length for blue light ($\lambda = 412$ and $\lambda = 440$ nm) is $\sim 50 \div 55$ m; the average attenuation length is ~ 30 m. These values are extremely good when compared to published seawater attenuation values obtained in conditions of collimated beam and detector geometry (3). The measured blue light attenuation length value is very close to the ones measured by Khanaev and Kuleshov (15) in the NESTOR site (16).

On the contrary, our results cannot be compared to the ones published by Bradner et al. (17) for the DUMAND project, Anassontzis et al. (18) for NESTOR and the ones measured by the ANTARES collaboration (19). These

Table 2

Values of Δa_{corr} and Δc_{corr} measured in the interval of depth 2850 ÷ 3250 m in *Alicudi* and *Ustica* during November-December 1999. Negative values, when statistically significant, are due to the dependence of water optical properties on salinity and temperature.

coefficient	Alicudi-1	Alicudi-2	Ustica-1	Ustica-2
	$\cdot 10^{-3}[m^{-1}]$	$\cdot 10^{-3}[m^{-1}]$	$\cdot 10^{-3}[m^{-1}]$	$\cdot 10^{-3}[m^{-1}]$
a412	12.3 ± 0.6	12.4 ± 0.5	17.8 ± 0.8	14.2 ± 0.5
c412	23.6 ± 1.8	23.3 ± 1.7	28.5 ± 1.7	22.8 ± 2.0
a440	10.1 ± 0.5	9.9 ± 0.5	13.2 ± 0.6	10.9 ± 0.5
c440	18.1 ± 1.8	17.8 ± 1.7	19.8 ± 1.8	17.7 ± 1.9
a488	4.4 ± 0.4	4.3 ± 0.4	5.5 ± 0.5	4.5 ± 0.5
c488	13.8 ± 1.8	13.7 ± 1.7	14.1 ± 1.6	14.2 ± 1.6
a510	-0.7 ± 0.4	-0.6 ± 0.3	0.4 ± 0.5	-0.2 ± 0.5
c510	0.6 ± 1.9	0.6 ± 1.7	0.4 ± 1.6	1.7 ± 1.6
a532	0.8 ± 0.4	1.2 ± 0.3	1.3 ± 0.5	1.2 ± 0.4
c532	-3.1 ± 1.9	-4.0 ± 1.7	-3.7 ± 1.6	-1.8 ± 1.8
a650	-3.1 ± 0.4	-2.5 ± 0.5	-2.6 ± 0.4	-1.8 ± 0.4
c650	15.7 ± 1.9	18.4 ± 1.9	16.2 ± 1.5	17.2 ± 1.7
a676	0 ± 0.5	0 ± 0.5	0 ± 0.5	0 ± 0.6
c676	3.7 ± 1.8	2.9 ± 1.6	5.6 ± 1.1	-0.9 ± 1.6
a715	-33. ± 1.0	-32. ± 1.0	-33. ± 1.0	-33. ± 1.0
c715	-33. ± 2.0	-33. ± 1.6	-33. ± 1.2	-33. ± 1.5

measurements were, indeed, carried out in conditions of not collimated geometry and the measured value is a quantity usually called *effective attenuation coefficient* $c_{eff}(\lambda)$. This quantity (an *apparent optical property*) is defined as the sum of absorption and only a fraction of the scattering coefficient:

$$c_{eff}(\lambda) = a(\lambda) + (1 - \langle \cos(\vartheta) \rangle) \cdot b(\lambda) \quad (19)$$

where $\langle \cos(\vartheta) \rangle$ is the average cosine of the volume scattering function distribution. This quantity strongly depends on the amount and dimension of the dissolved particulate. Measurements carried in ocean (6) gives $\langle \cos(\vartheta) \rangle \sim 0.95$. $c_{eff}(\lambda)$ for NEMO explored sites will be evaluated only after an *in situ* precise measurement of the volume scattering function scheduled for year 2001.

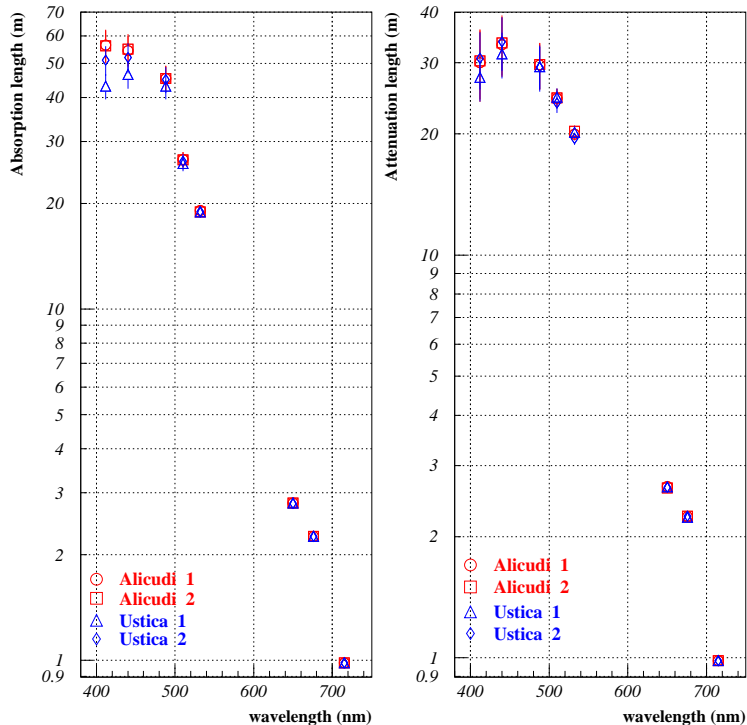


Fig. 7. Absorption and attenuation lengths as function of wavelength measured in *Alicudi* and *Ustica*, in the depth interval $2850 \div 3250$ m. The error bars include the systematic error.

9 Acknowledgements

The NEMO collaboration wants to thank M. Astraldi, G.P. Gasparini (Istituto di Oceanografia Fisica - CNR, La Spezia) and E. Accerboni, G. Gelsi, B. Manca, R. Mosetti (Istituto Nazionale di Oceanografia e Geofisica Sperimentale, Trieste), M. Leonardi (Istituto Sperimentale Talassografico - CNR, Messina) C. Viezzoli (SOPROMAR) for the fruitful collaboration. We want also to thank Captains V. Lubrano and M. Gentile, officers and crew of the *Urania* Oceanographic Research Vessel, for their outstanding experience and professionalism shown during the naval campaign.

References

- [1] M.A. Markov, *Proceedings of 10th Int. Conf. High Energy Physics*, Rochester, (1960).
- [2] M.A. Markov and I.M. Zheleznykh, *Nucl. Phys.*, **27** (1961) 385.
- [3] S.Q. Duntley, *J. Opt. Soc. Am.*, **53** (1963) 214.

- [4] S.G. Warren, *Applied Optics*, **23** (1984) 1206.
- [5] C.L. Braun and S. N. Smirnov, *J. Chem. Edu.*, **70** (1993) 612.
- [6] C.D. Mobley, *Light and Water*, Academic Press, San Diego (1994).
- [7] W.S. Pegau, D. Gray and J.R.V. Zaneveld *Applied Optics*, **36** (1997) 6035.
- [8] WETLabs, AC9 manual in www.wetlabs.com.
- [9] R.M. Pope and E.S. Fry, *Applied Optics*, **36** (1997) 33.
- [10] L.Kou, D. Labrie and P. Chylek *Applied Optics*, **32** (1993) 3531.
- [11] R.M. Pope *Optical absorption of pure water and sea water using the integrating cavity absorption meter, Ph.D. Thesis, Texas A&M, College Station* (1993).
- [12] M.S. Twardowski et al., *J. of Atm. and Ocean. Tech.*, **16** (1999) 691.
- [13] J.R.V. Zaneveld and J.C. Kitchen, *SPIE Vol. 2258 Ocean Optics XII*, **49** (1994).
- [14] R.C. Smith and K.S. Backer, *Applied Optics*, **20** (1981) 177.
- [15] S.A. Kanaev and A.P. Kuleshov, *Proceedings of the 3^d NESTOR Workshop*, Pylos (1983).
- [16] L.K. Resvanis, *Proceedings of the 3^d NESTOR Workshop*, Pylos (1983).
- [17] H. Bradner and G. Blackinton, *Applied Optics*, **23** (1984) 1009.
- [18] E.G. Anassontzis et al., *Nucl. Inst. Met.*, **A349** (1994) 242.
- [19] N. Palanque-Delabrouille, *Proceedings of the XXVI International Cosmic Ray Conference*, HE 6.3.20, Salt Lake City (1999).